

---

## The neurological principle: how traditional Chinese medicine unifies body and mind

---

Stefan Jaeger

National Library of Medicine,  
National Institutes of Health,  
Bethesda, MD 20894, USA  
E-mail: stefan.jaeger@nih.gov

**Abstract:** The unity of body and mind is an important concept in Chinese philosophy. Traditionally, the concept is informal and fuzzy, with no well defined meaning in the mathematical sense. This paper proposes a formal information-theoretical model for neural signal processing, arguing that physical principles are neural phenomena. For example, using the proposed model, the paper shows that time-dilation in Einstein's theory of relativity and Heisenberg's uncertainty principle can both be observed in neural signal processing. The paper therefore proposes a new concept, the neurological principle, which subsumes different natural principles. In particular, the paper shows that Yin and Yang, the two forces that according to Chinese philosophy pervade the universe and every entity therein, can be explained with the proposed model. These results provide Chinese medicine with a stronger mathematical foundation.

**Keywords:** neurological principle; Chinese medicine; body and mind; Yin-Yang; neural networks; information theory; learning; theory of relativity; uncertainty principle; anthropic principle; fine-structure constant; golden ratio; acupuncture.

**Reference** to this paper should be made as follows: Jaeger, S. (2013) 'The neurological principle: how traditional Chinese medicine unifies body and mind', *Int. J. Functional Informatics and Personalised Medicine*, Vol. 4, No. 2, pp.84–102.

**Biographical notes:** Stefan Jaeger is an NIH-Fellow in the United States National Library of Medicine (NLM) at the National Institutes of Health (NIH). He received his Diploma in Computer Science from University of Kaiserslautern and his PhD from University of Freiburg, Germany. He has held, among others, positions at Chinese Academy of Sciences, University of Maryland, University of Karlsruhe, and Daimler. His research interests include biomedical imaging, medical informatics, pattern recognition, machine learning, and Chinese medicine. He is an Associate Editor of *Electronic Letters on Computer Vision and Image Analysis*, and Editorial Board Member of *Quantitative Imaging in Medicine and Surgery*.

This paper is a revised and expanded version of a paper entitled 'An information-theoretic neural model based on concepts in Chinese medicine' presented at *Third Int. Workshop on Information Technology for Chinese*

## 1 Introduction

The unity, or oneness, of body and mind is an important concept in Asian philosophy. Seeing body and mind as two separate entities is usually considered as a symptom of illness, as in traditional medicine, or weakness, as in martial arts for example. This paper approaches the elusive body-mind concept in a more mathematical fashion. Elaborating on earlier work in Jaeger (2012a, 2012b), this paper presents a model that can explain phenomena both in our mind and in the physical world. Chinese medicine is an area in which traditional philosophical concepts go along with practical healing methods. This makes traditional Chinese medicine an ideal test bed for studies investigating the unity of body and mind. Acupuncture in particular is well suited to these studies because it is widely accepted and has a strong philosophical basis. On the other hand, the way it physically affects the nerves is not well understood yet. The traditional explanation for its efficacy is that acupuncture can correct imbalances and congestions in meridians, which are channels through which energy flows through the body. However, we are still lacking a deeper understanding of the neural processes underlying acupuncture. Modern approaches can only partly explain acupuncture so far (McIzack and Wall, 1965; James, 1977). Especially, the explanation of long-lasting memory effects is difficult. This paper will show that Yin and Yang, which are the two fundamental forces in Chinese philosophy, can be explained with the proposed information-theoretical model. Both forces play an important role in traditional Chinese medicine. The paper argues that the energy flowing through the meridians is nothing else but information in the mathematical sense (Shannon, 1948). Long-lasting effects can be achieved by learning the parameters of the proposed model, which describes the behaviour of a synapse. When the incoming information at a synapse matches the outgoing information, which is the central learning concepts put forward in this paper, harmony between Yin and Yang is achieved in the sense that the flow of information is neither congested nor empty.

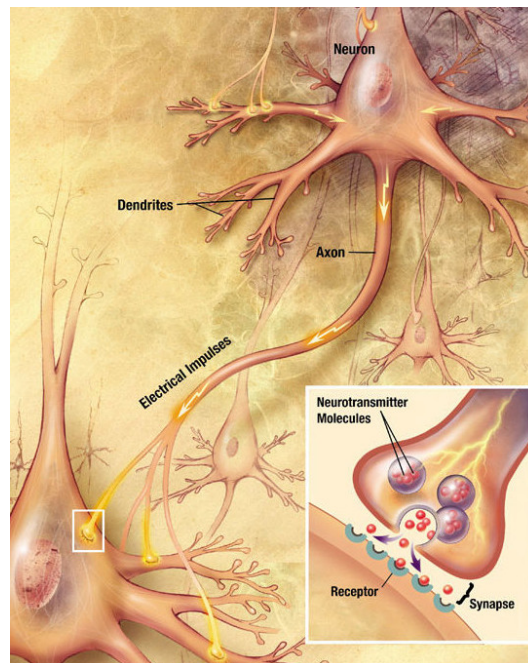
The paper is divided into the following sections: Section 2 gives a brief overview of the biology underlying the neurological model proposed here, explaining neurons and synapses in more detail. Section 3 introduces the linear information-theoretical model based on molecular concentrations measured at the presynaptic and postsynaptic terminal of a synapse. Section 4 first explains the fundamental forces of Yin and Yang before it shows that both forces can be described with an information-theoretical model. Section 5 presents several observations for the proposed model, indicating that many natural phenomena have a correspondence in our mind and in the way it works. Finally, the paper concludes with a summary of the main results.

## 2 Neural signal transmission

The human nervous system is composed of neurons, or nerve cells, which can communicate with each other via synapses. A synapse is a membrane-to-membrane

junction that allows either chemical or electrical signal transmission. In the case of chemical synapses, which will be in the focus here, signals are transmitted via neurotransmitters that can bridge the synaptic cleft, a small gap between the membranes of two nerve cells. As an illustration, the diagram in Figure 1 shows two neurons communicating with each other. In this figure, one neuron sends a signal to another neuron through its axon, which is a protrusion with potentially thousands of synapses and which can extend to other neurons in distant parts of the body. The other neuron typically receives the signal via its soma or so-called dendrites that conduct the received signal to the cell body (see Figure 1). In both cases, the signal needs to pass a synapse that transmits the signal by molecular means, via neurotransmitters, through the synaptic cleft, from the presynaptic terminal to the postsynaptic terminal. The small volume of the synaptic cleft allows neurotransmitter concentration to increase and decrease rapidly. Prior to any signal transmission, the neurotransmitters are enclosed in small spheres, synaptic vesicles, at the presynaptic terminal. On the other side, the postsynaptic terminal provides receptors for neurotransmitters travelling through the synaptic cleft. The lower right corner of Figure 1 shows a close-up of a synapse. The adult human brain contains between  $10^{14}$  and  $5 \times 10^{14}$  of these synapses. Synapses, and the way they transmit information, are crucial to the biological computations that underlie perception and thought. The common understanding is that synapses, and changes in their behaviour, are responsible for memorisation and human learning. To get insight into these processes, it is essential to study the molecular processes underlying signal transmission.

**Figure 1** A signal propagating down an axon to the cell body and dendrites of the next cell (see online version for colours)

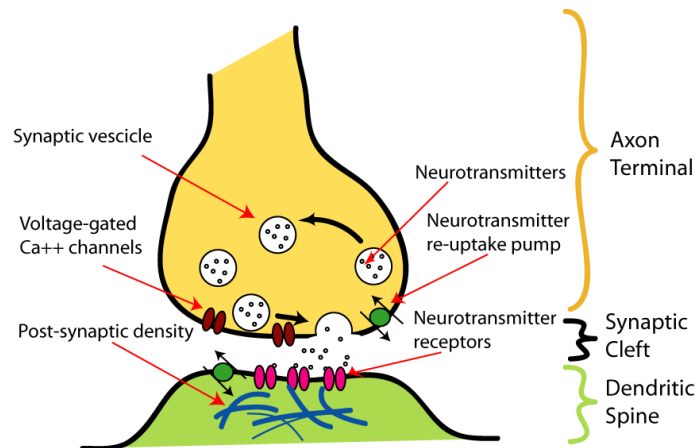


Source: NIA/NIH

The signal transmission at a (chemical) synapse happens in several steps (see Figure 2).

Except for the last step, each step takes no more than a fraction of a millisecond. The transmission is triggered by an electrochemical excitation (action potential) at the presynaptic terminal. The excitation causes calcium channels to open, allowing calcium ions to flow into the presynaptic terminal. The increased concentration of calcium ions in the presynaptic terminal causes the vesicles to release their neurotransmitters into the synaptic cleft. Some of these neurotransmitters bind to the receptors of the postsynaptic terminal, which opens ion channels in the postsynaptic membrane, allowing ions to flow into or out of the postsynaptic cell. This changes the transmembrane potential, leading to an excitation or inhibition of the postsynaptic cell. The action potential from the presynaptic terminal has thus created a postsynaptic potential by molecular means. Eventually, the docked neurotransmitters will break away from the postsynaptic receptors. Some of them will be reabsorbed by the presynaptic cell to initiate another transmission cycle.

**Figure 2** Signal transmission at a chemical synapse (see online version for colours)



Source: Julien (2005), Wikipedia – Surachit, Nrets

### 3 Neurological model

This section derives a linear model for the information processing performed by a synapse. The starting point is a well-known relationship for the sodium conductance at the cell membrane of a nerve cell. This is the same relationship that served as the starting point for the seminal paper by Hodgkin and Huxley (1952). In this paper, Hodgkin and Huxley proposed a set of equations explaining the electrical characteristics of nerve cells, and their underlying ionic mechanisms. Their model has been very successful, and has been used to simulate biological processes by computational means. Most notably are perhaps the different types of artificial neural networks that have been successfully applied to pattern recognition problems (Bishop, 1996; Hecht-Nielsen, 1990; McCulloch and Pitts, 1943; Minsky and Papert, 1972).

Sodium ions are largely responsible for generating action potentials in nerve cells. A nerve cell membrane has voltage-gated ion channels that are shut when the membrane is close to the resting potential. Once the membrane potential increases to a critical value, these ion channels open and allow sodium ions to pass the cell membrane and travel into the cell. The influx of sodium ions increases the membrane potential even more, causing more ion channels to open and thus allowing more sodium ions to move into the cell. This reinforcing process stops once the membrane potential has reversed and the nerve cell has reached its action potential. After reaching the action potential, the sodium channels close rapidly, preventing any more sodium ions to enter the cell. The sodium ions are then transported out of the nerve cell and the cell again returns to its resting potential. Understanding the temporal change of the sodium concentration is therefore important to understand the generation and transportation of action potentials.

In their mathematical model, Hodgkin and Huxley assume that the sodium conductance is proportional to the number of certain molecules on the inside of the membrane, but that the conductance is independent of the number of molecules on the outside. These molecules and their specific role are not important for the understanding of the subsequent text, so they will not be discussed further here. The paper confines itself to the important relationship between the inside and outside molecule concentrations, as stated in Hodgkin and Huxley (1952). According to Boltzmann's principle the proportion  $P_i$  of the molecules on the inside of the membrane is related to the proportion  $P_o$  on the outside by

$$\frac{P_i}{P_o} = \exp[(w + zeE)/kT], \quad (1)$$

where  $E$  is the potential difference between the outside and the inside of the membrane,  $w$  is the work required to move a molecule from the inside to the outside of the membrane when  $E = 0$ ,  $e$  is the absolute value of the electronic charge,  $z$  is the valency of the molecule (i.e., the number of positive electronic charges on it),  $k$  is Boltzmann's constant, and  $T$  is the absolute temperature (Hodgkin and Huxley, 1952). With  $P_i + P_o = 1$ , the expression for  $P_i$  becomes

$$P_i = \frac{1}{1 + \exp\left(-\frac{w + zeE}{kT}\right)}. \quad (2)$$

The concentration of the molecules on the inside of the membrane thus follows a sigmoid function  $S(x)$ , which has the following general mathematical form:

$$S(x) = \frac{1}{1 + e^{-\lambda x}}, \quad (3)$$

where input  $x$  is unbound and parameter  $\lambda$  controls the steepness of the function. Figure 3 shows  $S(x)$  for  $\lambda = 1$ ,  $\lambda = 2$ , and  $\lambda = 0.5$ . This relationship between sigmoid function and neural signal transduction has led to a widespread use of transfer functions with sigmoidal shapes in artificial neural networks, such as in feedforward/backpropagation networks for example (Bishop, 1996; Hecht-Nielsen, 1990).

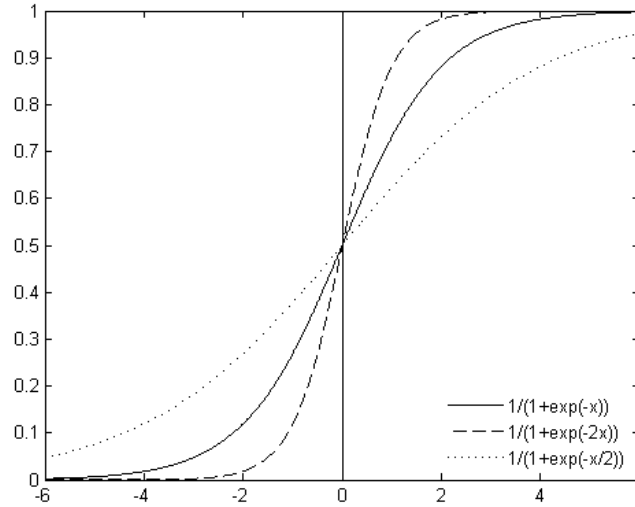
### 3.1 Linear information model

Concentrations will also play an important role in the model proposed in this paper. Instead of using sodium concentrations at the cell membrane, this paper uses calcium concentrations in the synaptic cleft and in the presynaptic terminal, as described in Section 2 and shown in Figure 2. The assumption is that the calcium concentration is directly correlated with the strength of the stimulus at the presynaptic terminal. In particular, the paper assumes that the ratio of the calcium concentration in the presynaptic terminal to the calcium concentration in the synaptic cleft determines the stimulus. Now, let  $p_i$  be the calcium concentration in the synaptic cleft. Then, the stimulus is given by the ratio  $(1 - p_i)/p_i$ . Furthermore, let  $p_o$  be the stimulus measured at the postsynaptic terminal. Obviously, we want  $p_o$  to be equal with the actual stimulus because this guarantees that we measure the correct stimulus at the postsynaptic terminal. When we resolve this requirement for  $p_i$ , we get the following result:

$$p_o = \frac{1 - p_i}{p_i} \quad (4)$$

$$\iff p_i = \frac{1}{1 + p_o} \quad (5)$$

**Figure 3** Sigmoid function for  $\lambda = 1$ ,  $\lambda = 2$ , and  $\lambda = 0.5$



If the change of  $p_o$  follows an exponential function, then equation (5) describes a similar sigmoid function as given by Hodgkin and Huxley for the concentration of sodium in equation (2). For  $p_o = p_i = p$ , which guarantees that the measured stimulus at the postsynaptic terminal equals the calcium concentration in the synaptic cleft, we can write the requirement in equation (4) as

$$p = \frac{1 - p}{p}. \quad (6)$$

For the learning process at the postsynaptic terminal, which is not understood well by the literature yet, the following learning mechanism is proposed: The information in the stimulus  $(1-p)/p$  at the presynaptic terminal is the input to a linear model, which measures information using the negative binary logarithm according to Shannon (1948). Mathematically, the proposed model can be written as follows:

$$I = -m \cdot \log_2 \left( \frac{1-p}{p} \right) + c, \quad (7)$$

where  $m$  and  $c$  are the slope and intercept of the linear model, respectively; and  $I$  is the learned information at the postsynaptic terminal. Learning is the process of aligning this information with the information in the measured concentration  $p$  by adjusting the parameters of the linear model, slope and intercept, so that the following requirement is met:

$$I = -p \cdot \log_2(p). \quad (8)$$

Thus, for  $c = 0$ , learning of the stimulus involves adjusting the slope  $m$ , so that  $m = p = (1-p)/p$ . For  $m = p$  and  $c = 0$ , the learned information  $I$  is then

$$I = -p \cdot \log_2 \left( \frac{1-p}{p} \right). \quad (9)$$

The main idea is that a neuron integrates over all outputs of its synapses, with each of its synapses processing information according to equation (7). Then, it sends the result to other neurons via its axon. The neuron thus essentially computes the entropy of its composite input.

### 3.2 Golden ratio

As outlined in the previous section, the calcium concentration  $p$  needs to satisfy the requirement in equation (6) so that the transmitted stimulus is equal to the measured concentration. In this case the information at the postsynaptic terminal, which is measured as  $-p \cdot \log_2(p)$ , is equal to the information in the input stimulus, which is  $-(1-p)/p \cdot \log_2((1-p)/p)$ . This happens when the concentration  $p$  satisfies the following requirement:

$$p = \frac{1-p}{p} \quad (10)$$

$$\implies p = \frac{\sqrt{5}-1}{2} \quad \text{or} \quad p = \frac{-\sqrt{5}-1}{2} \quad (11)$$

$$\implies p \approx 0.618 \quad \text{or} \quad p \approx -1.618. \quad (12)$$

According to equation (12), the measured concentration  $p$  equals the stimulus  $(1-p)/p$  for  $p \approx 0.618$ . This is the golden ratio, or strictly speaking the reciprocal  $\Phi$  of the golden ratio, which is typically symbolised by  $\varphi \approx 1.618$  (Livio, 2002; Huntley, 1970). For  $m = p = \Phi$  the intercept  $c$  in equation (7) is equal to zero. Therefore, learning of the intercept  $c$  is not necessary in this case. This could potentially explain why the golden

ratio is often preferred over other ratios in cognitive processes (Livio, 2002). According to the proposed linear model, the golden ratio can be perceived faster as it requires less learning. Interestingly, experiments in recent literature have confirmed that the golden ratio indeed plays a role in neural signal processing, thus supporting the proposed model (Weiss and Weiss, 2003; Pletzer et al., 2010).

#### **4 Yin and Yang**

According to Chinese philosophy, there are two opposing forces in the world, Yin and Yang (Miller, 2003; Watts, 1999). Yin and Yang are not only believed to be the foundation of our universe, but also to flow through and affect every being. Typical Yin-Yang opposites are for example night/day, cold/hot, rest/activity. Figure 4 shows the well-known black-and-white symbol of Yin and Yang.

**Figure 4** The common Yin-Yang symbol



We can see two intertwining spiral-like curves in Figure 4, which are actually semicircles in this simplified graphics, separating the Yin and Yang area. The small spots of different colour in each area symbolise that both Yin and Yang carry the seed of their opposites; Yin cannot exist without Yang, and Yang cannot exist without Yin. These spots will play no role in the following text. Neither will the assignment of black and white to Yin and Yang have any significance here, though Yin is typically associated with black and Yang with white. Contemporary literature has been mostly neglecting the graphical aspects of the Yin-Yang symbol, paying more attention to philosophical questions. It turns out that the original Yin-Yang symbol is more complex than its modern representation as two semicircles suggests (Browne, 2007; Graf, 1994). The Yin-Yang symbol has its origin in the I-Ching; one of the oldest and most fundamental books in Chinese philosophy (Tian and Tian, 2004; Hardaker, 2001). The symbol is tightly connected with the annual cycle of the earth around the sun, and the four seasons resulting from it. To investigate this cycle, the ancient Chinese used a pole that they put up orthogonally to the ground, as shown in Figure 5. With this setup, the ancient Chinese were able to record precisely the positions of the sun's shadow and divide the year into different sections. They measured the shortest shadow during the summer solstice, and measured the longest shadow during the winter solstice. After connecting the measured points and dimming the part that reaches from summer solstice to winter solstice (Yin), they arrived at a chart like the one in Figure 6. The resemblance between this chart and

the modern Yin-Yang symbol in Figure 4 is striking. Figure 6 provides visual evidence that the original Yin-Yang symbol describes the change of a pole's shadow length during a year. In fact, by rotating the chart and positioning the winter solstice at the bottom, the Yin-Yang chart of the ancient Chinese becomes very similar to the modern Yin-Yang symbol depicted in Figure 4. The white area of the Yin-Yang symbol is typically called Yang. It begins at the winter solstice and indicates a beginning dominance of daylight over darkness, which is the reason why the ancient Chinese associated it with the sun (or male). Accordingly, the dark area of the Yin-Yang symbol represents Yin, which begins with the summer solstice. Yin indicates a beginning dominance of darkness over daylight. The ancient Chinese therefore associated it with the moon (or female).

**Figure 5** Shadow model (see online version for colours)

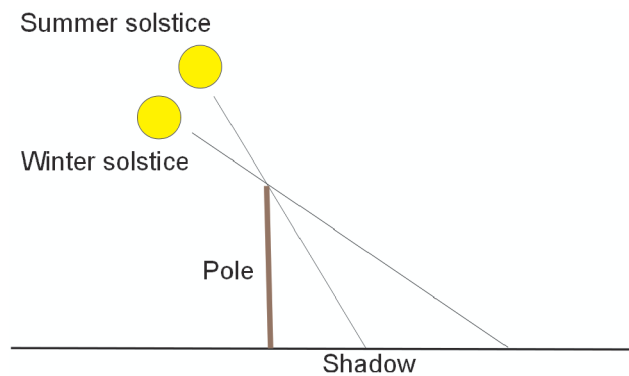
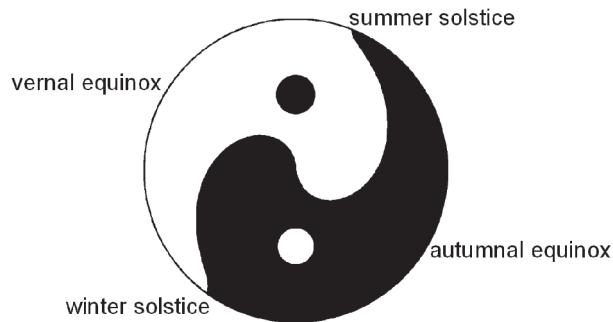


**Figure 6** Yin-Yang symbol for latitude  $L = 68^\circ$  (near polar circle) with equinoxes and solstices



#### 4.1 Daylight model

The rendering method for the Yin-Yang symbol presented here is based on daylight hours, which are connected with shadow lengths (Jaeger, 2012a). A long day has the sun standing high on the horizon at noon, casting a short shadow. On the other hand, a short day is the result of the sun standing low on the horizon at noon, producing a long

shadow. For computing the daylight time for a given day in the year, this section uses the formula given in Forsythe et al. (1995) and Jaeger (2012a). The formula takes many different factors into account, most notably the refraction of the earth's atmosphere. The daylight model presented here is therefore an accurate description of the actual daylight measurement of an observer on the ground. A detailed investigation of the formula is beyond the scope of this paper, though. The formula requires two input parameters, namely the day  $J$  of the year and the latitude  $L$  of the observer's location. It consists of three parts. The first part computes an intermediate result  $P$ , which is the input to the second part  $D'$ , which in turn is input to the third part  $D$  that provides the final result. The equation for the first part is:

$$P = \arcsin[0.39795 * \cos(0.2163108 + 2 * \arctan\{... \\ ... 0.9671396 * \tan[0.00860(J - 186)]\})]. \quad (13)$$

Given  $P$ , the second and third part compute the actual day length  $D$  in terms of sunshine hours as follows:

$$D' = \arccos \left\{ \frac{\sin\left(\frac{0.8333 * \pi}{180}\right) + \sin\left(\frac{L * \pi}{180}\right) * \sin(P)}{\cos\left(\frac{L * \pi}{180}\right) * \cos(P)} \right\} \quad (14)$$

$$D = 24 - \left(\frac{24}{\pi}\right) * D'. \quad (15)$$

Using these equations, Figure 7 shows the daylight time for each day of the year and for a latitude of  $68^\circ$ . This latitude is close to the polar circle, or Arctic Circle, in the northern hemisphere. The equivalent latitude in the southern hemisphere is the Antarctic Circle. The Arctic Circle marks the southernmost latitude in the northern hemisphere where the sun shines for 24 hours at least once per year (midnight sun) and does not shine at all at least once per year. Theoretically, the Arctic Circle marks the area where these events occur exactly once per year, namely during the summer and winter solstices. However, due to atmospheric refractions and because the sun is a disk rather than a point, the actual observation at the Arctic Circle is different. For example, the midnight sun can be seen south of the Arctic Circle during the summer solstice. According to Figure 7, the midnight sun shines for about 50 days at latitudes around  $68^\circ$ . Figure 8 shows the daylight hours in Figure 7 as a polar plot. In this polar plot, the distance to the origin stands for the daily sunshine hours. One full turn of  $360^\circ$  corresponds to one year. There is one important difference to Figure 7, though. For the second half of the year, Figure 8 shows the hours of darkness instead of the daylight hours. The number of hours with darkness is simply the full day length of 24 hours minus the number of daylight hours. Drawing the daylight hours in such a way produces the two spirals depicted in Figure 8. Coloring the areas delimited by both spirals and the outer circle in black and white then produces a rotated version of the Yin-Yang symbol in Figure 6. For latitudes around the polar circle, the spirals in Figure 8 originate either directly in the origin of the polar plot or in a point close to it. This is because there will be at least one day with no sunshine.

Figure 9 shows a Yin-Yang symbol generated with the daylight model for  $L = 68^\circ$  (same symbol as in Figure 6). The symbol is rotated counter-clockwise so that the x-axis is vertical. Both spots lie on the now vertical x-axis, plotted halfway between the polar plot's origin and the outer circle.

4.2 *Information-theoretical Yin-Yang model*

The mathematical formulation of the Yin-Yang symbol given in equations (13)–(15) is clumsy. This section presents a more concise description of the Yin-Yang symbol. It shows that a linear information-theoretical model can approximate the Yin-Yang symbol with an average error of less than 1% with respect to the day length. In order to do so, the paper measures the Shannon information, which is the negative binary logarithm ( $-\log_2(p)$ ) of a probability value  $p$  (Shannon, 1948). The model proposed here has the following form:

$$\Theta(p) = -\pi \times \log_2(p) \tag{16}$$

$$r(p) = -24 \times \log_2(p), \tag{17}$$

**Figure 7** Daylight hours for latitude  $L = 68^\circ$  (near polar circle) (see online version for colours)

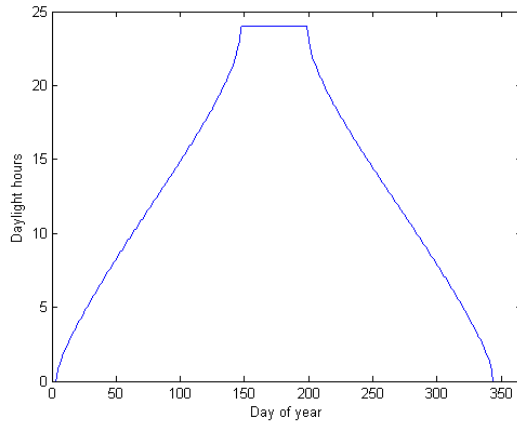


**Figure 8** Polar daylight plot for latitude  $L = 68^\circ$  (near polar circle) (see online version for colours)

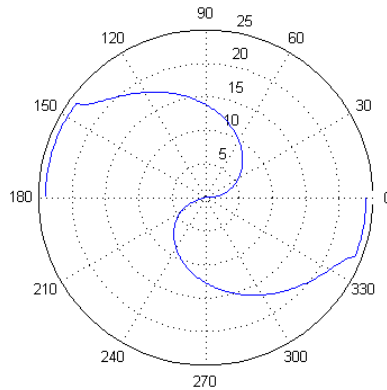
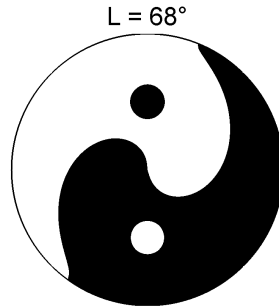


**Figure 9** Yin-Yang symbol generated with the daylight model for  $L = 68^\circ$



where  $\Theta(p)$  and  $r(p)$  are the angular and radial coordinates, respectively, and  $p \in [0.5, 1]$  is the model's input. Both equations can be summarised in one equation:

$$\Theta(p) = \frac{\pi}{24} \times r(p). \tag{18}$$

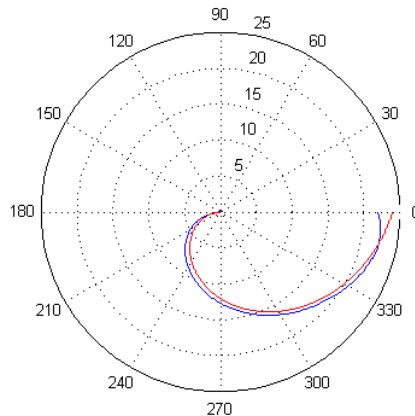
Note that the model's input range is the output range of the sigmoid function for positive input. In the neural context of Section 3, the model input would be the measured calcium concentration in the synaptic cleft (see equation (5)).

Figure 10 shows the approximation of one branch of the Yin-Yang symbol for  $L=68^\circ$  (red curve), obtained when applying equation (18).

The figure also shows the original branch computed with equations (13)–(15) (blue curve). We see that this approximation of the Yin-Yang symbol already provides a very close model for the symbol. The model given by equation (18) can be further improved by using a linear regression, exploiting the linear relationship between the angular and the radial coordinate. Let

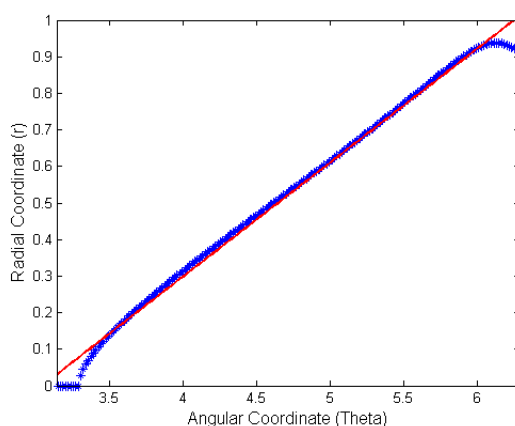
$$\Theta(p) = mr(p) + c \tag{19}$$

**Figure 10** Approximation of one branch of the Yin-Yang symbol for  $L=68^\circ$  (close to polar circle) with a linear information model (red) (see online version for colours)



be the general form of the linear information model for the Yin-Yang symbol, where  $m$  is the slope,  $c$  is the offset or intercept, and  $r(p)$  is a logarithmic function of the input. Accordingly, the linear approximation has the form  $\Theta' = m'r + c'$ , where  $m'$  and  $c'$  are the slope and intercept of the regression line, respectively. Figure 11 shows the optimal regression line (red) obtained for the Yin-Yang branch (blue) shown in Figure 10. Note that the range of the angular coordinate is  $[\pi, 2\pi]$  and the radial coordinate has been normalised to  $[0, 1]$ , showing the normalised day length with the daylight hours of each day divided by 24. As we can see in Figure 11, the red regression line provides an almost perfect fit. Only toward the limits of the angular range does the linear information model differ from the original Yin-Yang model. This is largely due to numerical problems of the function approximation. With  $m' \approx 0.134$  and  $c' \approx 3$ , the mathematical equation for the regression line is

**Figure 11** Linear regression line (red) for a branch (blue) of the Yin-Yang symbol at  $L = 68^\circ$  (close to polar circle) (see online version for colours)



$$\Theta'(p) = 0.134r(p) + 3, \quad (20)$$

or, in another form stressing that  $\Theta'$  is indeed a linear function of information:

$$\Theta'(p) = 3 - 3.2 \cdot \log_2(p). \quad (21)$$

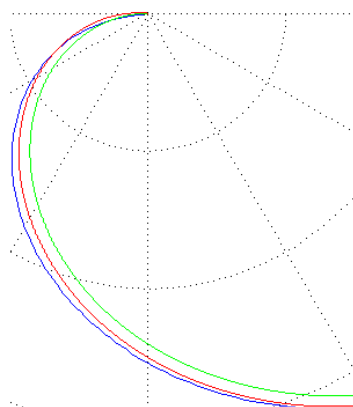
The median error of this model is 0.23, which is less than 1% with respect to a day length of 24 hours. Figure 12 shows a close-up of all approximations in one figure.

The original Yin-Yang branch is again shown in blue. The first rough approximation of equation (18) is shown in green, and the optimal linear regression model is shown in red. We can see that the linear regression model lies between the rough approximation (green) and the Yin-Yang branch (blue), and we can see that it is much closer to the Yin-Yang branch.

The equations derived in this section for Yin and Yang are based on the same linear information-theoretical model presented in Section 3. The same model can thus describe neurological as well as physical phenomena. Moreover, learning the parameters of the model has a geometrical interpretation. According to equations (18) and (21), changing

the slope  $m$  is equivalent to changing the radius of the Yin-Yang symbol, which is 24 hours in the daylight model. Furthermore, changing the intercept  $c$  translates to a rotation of the Yin-Yang symbol.

**Figure 12** Approximation of one branch of the Yin-Yang symbol for  $L = 68^\circ$  (close to polar circle) with a linear model (green) and a linear regression model (red) (see online version for colours)



## 5 Neurological principle

This section presents several theoretical observations that support the main thesis of this paper, namely that several fundamental principles in nature are actually instantiations of an even more fundamental principle. For lack of a better name, the principle is called neurological principle in this paper. The main claim of the neurological principle is that all natural principles are related to neural signal processing. Physical objects thus become the result of our thinking, a product of our mind and its cognitive activities. Furthermore, natural laws become expressions of the operation and limitations of neural signal processing, in particular the signal transmission at synapses, as explained above. The following subsections will show that many well-known natural principles are consistent with the neural model explained in Section 3. In fact, the proposed neural model subsumes these principles, supporting the argument of a more fundamental principle. In particular, this section will show that the relativistic principle, the uncertainty principle, and the anthropic principle are all different expressions of the neurological principle.

### 5.1 Relativistic principle

The relativistic principle goes back to the seminal work of Einstein, in particular to his theory of relativity (Einstein, 1995). Einstein, starting with his famous assumption that the speed of light is constant, derived several fundamental results. The most well-known claim is that it is not possible to travel faster than the speed of light. Another related claim of his theory of relativity is the so-called time dilation. According to Einstein's

theory of relativity, every system moving relative to an observer will show a slower lapse of time compared to the observer. The faster the system moves, the slower the observer will see the time pass within the system. In his general theory of relativity, Einstein extended time-dilation to objects experiencing acceleration and gravitation. The observed time in the frame of references of these objects will also pass slower. Einstein's theory of relativity has stood the test of time so far, and has been confirmed by numerous practical experiments.

Mathematically, time dilation can be described using the Lorentz factor, or actually the inverse Lorentz Factor, in equation (22):

$$t' = \sqrt{1 - \left(\frac{v}{c}\right)^2} \times t, \quad (22)$$

where  $t$  is the time measured by an observer, i.e., elapsed time intervals in the observer's own frame of reference, and  $t'$  is the elapsed time measured by the observer for a system moving relative to him. The constant  $c$  denotes light speed and the parameter  $v$  is the speed of the moving system. The ratio  $v/c$  is thus the relative velocity of the moving system with respect to light speed. We can see that  $t'$  approaches zero for increasing speed. The observer thus sees a dilation of time for systems approaching light speed, and measures no lapse of time for a system moving at the exact speed of light. The Lorentz factor plays an important role in Einstein's theory of relativity, and is important not only for explaining time dilation. It also describes how mass and length change for a system whose velocity approaches the speed of light. With increasing speed, an observer will also measure a shorter length and a larger mass for the moving object. According to the Lorentz factor, these relativistic effects become more pronounced as the moving object approaches the speed of light. At the speed of light, the observer would measure no time lapse, no length, and an infinite mass for the moving object.

When we look again at the neural model proposed above, we can see similarities. According to Section 3, the stimulus and the measured concentration  $p$  are identical when  $p$  satisfies the following requirement (see also equation (6)):

$$p = \frac{1-p}{p} \quad (23)$$

$$\iff p = 1 - p^2. \quad (24)$$

Using the basic linear equation of the proposed model,  $K = -E \cdot \log_2(p)$ , with  $E = p = (1-p)/p$ , we obtain the following derivation for  $K$ :

$$K = -(1-p) \times \log_2(p)/p \quad (25)$$

$$\stackrel{(24)}{\iff} K = -p \times \log_2(1-p^2) \quad (26)$$

$$\iff K = -p \times \log_2\left(\sqrt{1-p^2}\right) \cdot 2. \quad (27)$$

Note the Pythagorean relationship between the measured value  $\sqrt{1-p^2}$ , which is the argument of the logarithm, and the slope  $p$ . Due to this Pythagorean relationship, the perceived stimulus  $(1-p)/p$  and the measured concentration  $p$  become now mathematically indistinguishable, and thus replaceable. According to the biological motivation in Section 2 and the neurological model in Section 3, the measured stimulus

depends on the concentration of calcium ions in the presynaptic terminal. The larger the concentration, the larger the stimulus. However, the larger the stimulus, the more time needs to pass in order to allow more calcium ions to flow through the open ion channels of the nerve cell. Thus, the measured stimulus is directly correlated with time, and  $\sqrt{1-p^2}$  indeed represents time. Moreover, for  $p = 1$ , the calcium concentration in the synaptic cleft will be the highest and the calcium ions will flow quickly into the presynaptic terminal due to the large concentration difference. Thus,  $p$  can be considered as the relative speed of the calcium ions, with  $p = 1$  being the maximum speed corresponding to light speed in the physical world. It is interesting to note here that physicists sometimes normalise the light speed  $c$ , which is about 300,000,000 meter per second, so that the maximum speed becomes one. They do this by using so-called Planck units. If we look at equation (27), we can see that speed  $p$  is one if the measured time is zero ( $\sqrt{1-p^2} = 0$ ). Conversely, if the measured time is one, which means one unit of time has elapsed, then the corresponding speed  $p$  is zero. This is in accordance with the time dilation predicted by Einstein's theory of relativity. Furthermore, in the case of  $\sqrt{1-p^2} = 0$  and  $p = 1$ , the information or energy  $K$  will be infinite, which is again in accordance with the theory of relativity.

## 5.2 Uncertainty principle

The second principle investigated here is the uncertainty principle introduced by Heisenberg. In contrast to Einstein's theory of relativity, which deals with large-scale phenomena, Heisenberg's uncertainty principle pertains to quantum physics. In the quantum mechanical world, the idea that we can locate objects exactly breaks down. Heisenberg's uncertainty principle states that locating a particle in a small region of space makes the momentum of the particle uncertain; and conversely, that measuring the momentum of a particle precisely makes the position uncertain. For instance, let  $\Delta x$  be the uncertainty about the exact location of an electron, and let  $\Delta p$  be the dispersion of its momentum. Then, Heisenberg's uncertainty principle can be formulated as follows:

$$\frac{\hbar}{2} \leq \Delta x \times \Delta p, \quad (28)$$

where  $\hbar$  is the reduced Planck constant. This means that the combination of the error in position times the error in momentum is always greater than a positive constant. From this it follows that we cannot simultaneously find both the position and momentum of an electron to arbitrary accuracy. The more precisely we determine the position of the electron, the less we will know about its momentum; conversely, the more we know about the momentum, the less we will know about the position of the electron. This uncertainty of an electron's position and momentum is established the moment it is observed, resulting in the measured values being dispersed.

Now, let us again compare the uncertainty principle with the equations derived in the previous subsection, in particular with equation (27). The following derivation of equation (27) into an inequality produces a result similar to the uncertainty principle in equation (28):

$$K = -p \times \log_2 \left( \sqrt{1-p^2} \right) \cdot 2 \quad (29)$$

$$\implies K \leq -\log_2 \left( \sqrt{1-p^2} \right) \cdot 2 \quad (30)$$

$$\implies \frac{1}{2} \leq -\log_2(\sqrt{1-p^2}) \cdot K^{-1}. \quad (31)$$

Equation (31) states that the product of our observed information  $-\log_2(\sqrt{1-p^2})$  and the inverse information  $K$  is always equal to or greater than  $1/2$ . This imposes a severe limitation to what we can measure. On one hand, we want the uncertainty in our measured value  $-\log_2(\sqrt{1-p^2})$  to be zero, which means we have a strong unambiguous stimulus. On the other hand, we want  $K$  to be as large as possible because this effectively means that  $p=1$  and that the uncertainty we measure,  $-\log_2(\sqrt{1-p^2})$ , is equal to the uncertainty  $K$  that we learn by means of the linear model. However, equation (31) tells us that having both is not possible.

We can even observe a connection with location and momentum, as in Heisenberg's original uncertainty principle. The information  $K$  is the product of velocity and energy (see Section 5.1) and can thus be considered as momentum. For  $\sqrt{1-p^2}=1$ , the uncertainty  $-\log_2(\sqrt{1-p^2})$  will be zero. This is related to location because if the measured stimulus is maximum, all calcium ions will be evenly distributed in the synaptic cleft and in the presynaptic terminal, so there will be no uncertainty regarding their location. Consequently, analogous to Heisenberg's original uncertainty principle, equation (31) tells us that we cannot measure both location and momentum without uncertainty.

### 5.3 *Anthropic principle*

The last principle in this paper brings us back to the Yin-Yang model derived in Section 4.2. The anthropic principle states that the physical universe must be compatible with the life observing it in the sense that the universe provides the right parameters for life to thrive. Otherwise, life could not emerge and no observer could perceive the surrounding universe. As a direct consequence, the anthropic principle claims that natural constants must be compatible with life, and that finding constants to be compatible with life is not surprising at all. A typical example is the fine-structure constant, which is a measure of the strength of the electromagnetic force, controlling the interaction between electrically charged elementary particles, such as electrons and light photons. The fine-structure constant is thus directly related to light emission. It has no dimension, which means that it is a constant that keeps its numerical value under different units. According to the latest measurements, the current value of the fine-structure constant *alpha* is about  $7.2973525698 \times (10^{-3})$ , which is approximately  $1/137$ . Following the reasoning of the anthropic principle, the next paragraph argues why the fine-structure constant has exactly this value (The paragraph is a quote from Barrow (2001)).

“The anthropic principle is a controversial argument of why the fine-structure constant has the value it does: stable matter, and therefore life and intelligent beings, could not exist if its value were much different. For instance, were  $\alpha$  to change by 4%, stellar fusion would not produce carbon, so that carbon-based life would be impossible. If  $\alpha$  were  $> 0.1$ , stellar fusion would be impossible and no place in the universe would be warm enough for life as we know it.”

Given that the fine-structure constant  $\alpha$  is related to light emission, it is perhaps not so surprising that it emerges in the Yin-Yang daylight model, which was presented in Section 4 and linearly approximated in Section 4.2. When we compute the slope  $m$  in equations (19) and (20) for  $L = 67^\circ$ , which is near the polar circle, then we can observe the following relationship between  $m$  and the fine-structure constant  $\alpha$ :

$$m \approx \frac{1}{\alpha \cdot 1024}. \quad (32)$$

In this case, the absolute error between  $m$  and  $1/(\alpha \times 1024)$  is less than  $3 \times 10^{-4}$ , which is very small compared to the uncertainty of the approximation model used. Therefore, we could replace the slope  $m$  given by the model with the new value  $1/(\alpha \times 1024)$  without introducing too much error. The multiplying scalar of 1024 would then essentially mean that we measure information in kilobits (kibits).

## 6 Conclusion

This paper proposes a linear information-theoretical model for neural signal processing. Based on this model, the paper offers new explanations for several natural phenomena and principles, including Einstein's theory of relativity and Heisenberg's uncertainty principle. In the context of Chinese medicine, the proposed model provides the forces of Yin and Yang with a formal definition, thus confirming the importance of seemingly informal concepts in this discipline. Moreover, under the given formalisation of Yin and Yang, statements claiming that traditional healing methods affect Yin and Yang become meaningful. In fact, the paper claims that acupuncture directly affects these forces, and that it is mathematically equivalent to a rotation and/or resising of the Yin-Yang symbol. This is the first acupuncture model that refers directly to the proper formal definition of Yin and Yang. The proposed model is based on the idea that neural learning processes happen mainly at synapses. Learning is achieved when the information in the input stimulus equals the information measured at the postsynaptic terminal. However, learning has theoretical limitations, as manifested in a relationship similar to Heisenberg's uncertainty principle for example. The paper subsumes these learning phenomena in the neurological principle, which claims that all natural laws have a direct correspondence in the human cognitive processes and mind. The paper thus assigns the human mind a prominent place. This is in contrast to the anthropologic principle, which rather claims that human rational thinking is the result of nature. In fact, the paper claims that body and mind are essentially the same because the natural phenomena are the result of our cognitive processes and their limitations. In summary, the paper has brought forward model observations supporting this thesis, in particular a time dilation as in Einstein's theory of relativity, and an uncertainty principle similar to Heisenberg's uncertainty principle. Furthermore, the paper claims that Yin and Yang can describe neurological as well as physical phenomena. In addition, the paper shows that the fine-structure constant, or at least a constant very close to the fine-structure constant, plays an important role in the model presented. Given these observations, the hope is that the proposed model helps to get a better understanding of traditional healing methods.

## References

- Barrow, J. (2001) 'Cosmology, life, and the anthropic principle', *Annals of the New York Academy of Sciences*, Vol. 950, No. 1, pp.139–153.
- Browne, C. (2007) 'Taiji variations: Yin and Yang in multiple dimensions', *Computers & Graphics*, Vol. 31, No. 1, pp.142–146.
- Bishop, C.M. (1996) *Neural Networks for Pattern Recognition*, Oxford University Press, USA.
- Einstein, A. (1995) *Relativity: The Special and the General Theory*, Three Rivers Press, Reprint Edition, New York.
- Forsythe, W., Rykiel, E., Stahl, R., Wu, H-I. and Schoolfield, R. (1995) 'A model comparison for daylength as a function of latitude and day of year', *Ecological Modelling*, Vol. 80, No. 1, pp.87–95.
- Graf, K-D. (1994) 'Mathematics and informatics in old symbols: tai chi symbol and hexagrams from the I Ging', in Yokochi, K. and Okamori, H. (Eds.): *Proceedings of the Fifth Five Nations Conference on Mathematics Education*, Osaka, Japan, pp.15–21.
- Hardaker, C. (2001) 'The hexagon, the solstice and the kiva', *Symmetry: Culture and Science*, Vol. 12, Nos. 1–2, pp.167–183.
- Hecht-Nielsen, R. (1990) *Neurocomputing*, Addison-Wesley, USA.
- Hodgkin, A. and Huxley, A. (1952) 'A quantitative description of membrane current and its application to conduction and excitation in nerve', *The Journal of Physiology*, Vol. 117, No. 4, pp.500–544.
- Huntley, H. (1970) *The Divine Proportion*, Dover Publications, New York.
- Jaeger, S. (2012a) 'A geometical approach to chinese medicine: the origin of the Yin-Yang symbol', in Kuang, H. (Ed.): *Recent Advances in Theories and Practice of Chinese Medicine*, InTech, pp.29–44.
- Jaeger, S. (2012b) 'An information-theoretic neural model based on concepts in Chinese medicine', *Third Int. Workshop on Information Technology for Chinese Medicine, IEEE Int. Conf. on Bioinformatics and Biomedicine (BIBM)*, Philadelphia, USA, pp.496–502.
- James, B. (1977) 'Mechanism of acupuncture analgesia', *British Medical Journal*, Vol. 1, No. 6059, pp.512–512.
- Julien, R. (2005) *A Primer of Drug Action: A Comprehensive Guide to the Actions, Uses, and Side Effects of Psychoactive Drugs*, Worth Publishers, New York, pp.60–88.
- Livio, M. (2002) *The Golden Ratio*, Random House, Inc, New York.
- McCulloch, W.S. and Pitts, W.A. (1943) 'A logical calculus of ideas immanent in nervous activity', *Math. Biophysics*, Vol. 5, pp.115–133.
- Melzack, R. and Wall, P. (1965) 'Pain mechanisms: a new theory', *Science*, Vol. 150, pp.971–978.
- Miller, J. (2003) *Daoism: A Short Introduction*, Oneworld Publications, Oxford.
- Minsky, M. and Papert, S. (1972) *Perceptrons: An Introduction to Computational Geometry*, 2nd ed., The MIT Press, Cambridge, MA.
- Pletzer, B., Kerschbaum, H. and Klimesch, W. (2010) 'When frequencies never synchronize: the golden mean and the resting EEG', *Brain Research*, Vol. 1335, pp.91–102.
- Shannon, C.E. (1948) 'A mathematical theory of communication', *Bell System Tech. J.*, Vol. 27, Nos. 623–656, pp.379–423.
- Tian, H. and Tian, F. (2004) *The True Origin of Zhou Yi (in Chinese)*, Shanxi Science and Technology Publishing House, China.
- Watts, A. (1999) *The Way of Zen*, Vintage, New York.
- Weiss, H. and Weiss, V. (2003) 'The golden mean as clock cycle of brain waves', *Chaos, Solitons & Fractals*, Vol. 18, No. 4, pp.643–652.